



ELSEVIER

Available online at www.sciencedirect.com

SCIENCE @ DIRECT®

Journal of Electrostatics 61 (2004) 223–230

Journal of
ELECTROSTATICS

www.elsevier.com/locate/elstat

Flow visualization and current distributions for a corona radical shower reactor[☆]

Seishu Shimamoto^a, Seiji Kanazawa^{a,*}, Toshikazu Ohkubo^a,
Yukiharu Nomoto^a, Jerzy Mizeraczyk^b, Jen-Shih Chang^c

^a *Department of Electrical and Electronic Engineering, Faculty of Engineering, Oita University, 700
DannoHaru, Oita 870-1192, Japan*

^b *Centre for Plasma and Laser Engineering, Institute of Fluid Flow Machinery, Polish Academy of Sciences,
Fiszera 14, 80-231 Gdańsk, Poland*

^c *Department of Engineering Physics, Faculty of Engineering, McMaster University, Hamilton, Ont,
Canada L8S 4M1*

Received 28 June 2003; accepted 15 February 2004

Abstract

NO_x removal in a corona radical shower system depends not only on the discharging characteristics but also on the airflow pattern in the reactor. In this paper, the effects of discharging nozzle electrode configuration such as number of nozzles on the pipe electrode on the current distribution and airflow in the reactor are measured. The airflow in the reactor is visualized for the several nozzle electrode configurations by Shadowgraph method. As a result, it is found that the current density distribution depends on the nozzles configuration on the pipe electrode, and corona current density increase with increasing the applied voltage, while the location of maximum current density reaches to the underneath the tip of the nozzles as the applied voltage increases. The image obtained by Shadowgraph method shows the generation of turbulent flow around the pipe with nozzles electrode. It is found that the airflow is much different from that of the conventional discharging electrode such as the smooth wire.

© 2004 Elsevier B.V. All rights reserved.

Keywords: DC positive streamer corona; Ionic wind; Corona current density distribution; Flow; Visualization; Corona; Radical; Shower; Reactor

[☆] Presented at the 2003 Joint Meeting of the Electrostatics Society of America and the IEEE Industry Applications Society Electrostatic Processes Committee, June 24–27, 2003, Little Rock, AR, USA.

*Corresponding author. Tel.: +81-97-554-7828; fax: +81-97-554-7820.

E-mail address: skana@cc.oita-u.ac.jp (S. Kanazawa).

1. Introduction

Up to now, many researches have been made to remove NO_x in flue gases by using non-thermal plasmas [1–5]. A corona radical shower system (CRSS) has been considered to be one of the most efficient methods in terms of the energy efficiency for NO_x removal [6–8]. In CRSS, a pipe with nozzles electrode is used as a stresses electrode. Therefore, it is considered that the flow field in the vicinity of the discharge zone is complicated compared to that of the conventional one such as the wire-to-plate geometry [9,10]. Recently, NO density profiles obtained in our laser-induced fluorescence (LIF) measurements indicate that the electrohydrodynamic (EHD) flow plays the dominant role in the process when the gas velocity is low, and NO oxidation occurs not only in the vicinity of the discharging electrode but also in the region far from the discharge zone [11]. Moreover, according to the visualization of flow field in the CRSS reactor using laser light visualization method [12], the EHD-induced secondary flow (i.e. ionic wind) is responsible for the transportation of ozone in the direction of upstream of the reactor. As the EHD-induced secondary flow is correlated with the discharging characteristics, the current distribution seems to become an important factor affecting the processes [13,14]. Especially, the current distribution can be controlled by changing the nozzle configuration such as the number of the nozzles on the pipe electrode, nozzle-to-nozzle spacing, and nozzle arrangement. In this study, the effects of nozzle configuration on current distributions are measured. The airflow in the reactor is also visualized by Shadowgraph method. The relationship between the current distribution and airflow pattern is discussed to provide the information about the design of optimized CRSS.

2. Experimental apparatus and method

A schematic diagram of experimental apparatus is shown in Fig. 1. In order to observe corona discharge and airflow inside the reactor, the discharging electrode system is enclosed in acrylic vessel. In the CRSS, a pipe (4 mm in diameter) with nozzles (1.5 mm outer diameter, 1.0 mm inner diameter, 5 mm in length) electrode is used as a discharging electrode and has a function of additional gas injection. The pipe electrode is placed at the center of grounded parallel plates ($50 \times 12.5 \text{ cm}^2$) with a gap of 10 cm as shown in Fig. 1. The several nozzle configurations by changing the number of the nozzles on the pipe electrode, nozzle-to-nozzle spacing, and nozzle arrangement is evaluated. In this paper, the experimental results using the pipe with one pair of nozzles (2 nozzles) or five pairs of nozzles (10 nozzles) electrodes shown in Fig. 2 are presented.

An arrangement diagram of the current density measuring probe on the plate electrode is shown in Fig. 3. The diameter of the probe is 3 mm and each probe is electrically isolated from the plate electrode. The spacing of the probes is 5 mm. The corona currents flowing to the probe is measured by an electrometer. Current density is calculated from the corona current divided by the effective probe area

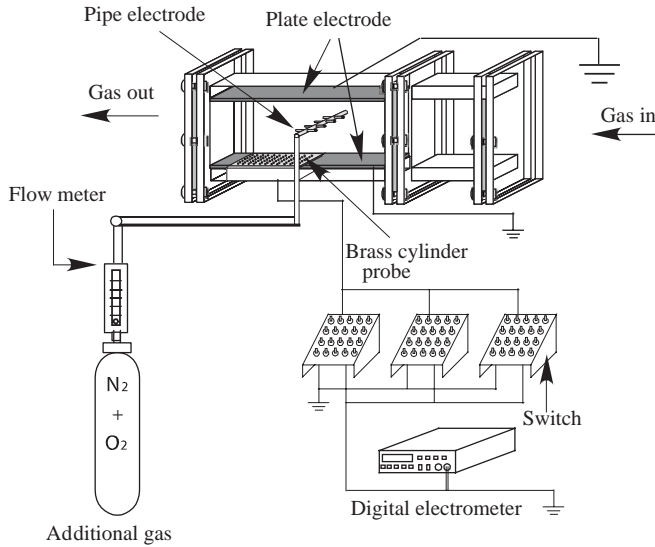


Fig. 1. Experimental set-up.

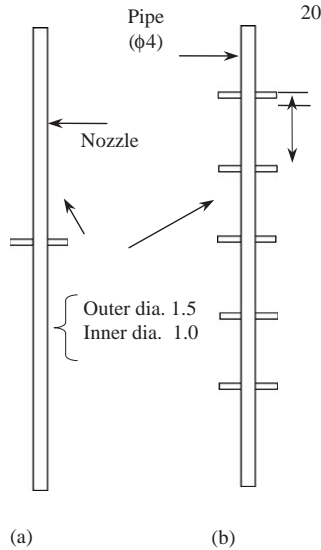


Fig. 2. Construction of discharging electrode (unit: mm). (a) 2 nozzles; (b) 10 nozzles.

(0.0962 cm²). The current density distribution is measurable in the parallel (*x*-axis) and vertical (*y*-axis) directions to the gas flow as shown in Fig. 3.

The airflow pattern inside the reactor is visualized by Shadowgraph method. The system consists of a halogen lamp and two concave mirrors (30 cm in diameter), and CCD camera with a video recorder. In order to make density gradient of airflow,

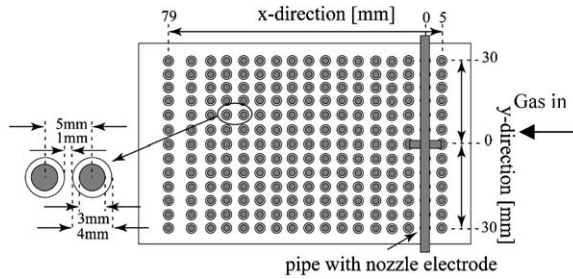


Fig. 3. Schematic of current probe on the plate electrode.

three nichrome wires (0.15 mm in diameter and 12.5 mm length) are set at 25 cm upstream of the discharging electrode. With the heated air through the wires (0.64 A/wire), the streamlines of the airflow between the stressed pipe with nozzles electrode and the grounded plate electrode can be observed. Laser light visualization method is also used for a detailed investigation.

Dry NO (200 ppm)/air mixture or only air is supplied to the reactor as a main gas. The main gas flow velocity (U_T) is 0.5 cm/s to 1 m/s by changing the gas flow rate. As an injection gas, the additional gases consisting of N_2 , O_2 , and CO_2 are introduced from the nozzles with an average velocity of 1.6–7.9 m/s. Positive dc high voltage is used to produce streamer coronas. The experiments are conducted at room temperature under atmospheric pressure.

3. Experimental results

3.1. Streamer corona discharge characteristics

The typical corona discharge current–voltage characteristic is shown in Fig. 4. The air containing NO (200 ppm) is introduced to the reactor at the flow rate of 5.0 L/min. The averaged main gas velocity is 6.7 mm/s. The corona onset voltage of this CRSS is 16.3 kV. Fig. 5 shows the comparison of discharge luminescence and the corona current density profiles at the plate electrode along x-axis ($y=0$). The corona current density increases with increasing the applied voltage, and the current flowing area spreads much wider than the discharge luminescence area. The low current region exists underneath the pipe electrode in both figures. Fig. 6 shows the corona current distribution on the plate electrode. As well as Fig. 5, high current density distribution area increases with increasing the applied voltage, while the points of maximum current density reach to the underneath the tip of the nozzles as the applied voltage increases. In the case of the pipe with one pair of nozzles, the corona current density distribution pattern is a sector as shown in Figs. 6(a) and (b). On the other hand, in the case of the pipe with five pairs of nozzles, the current distribution area increases compared to that of one pair of nozzles (Fig. 6(c)).

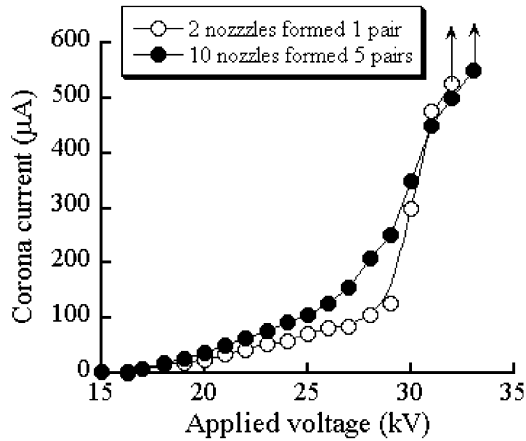


Fig. 4. Corona discharge current–voltage characteristic. Treatment gas: $N_2 + O_2 + NO$ ($NO: 200$ ppm, $O_2 = 20\%$), injection gas: $N_2 + O_2$ (19%) + CO_2 (4.76%) = 0.74 L/min.

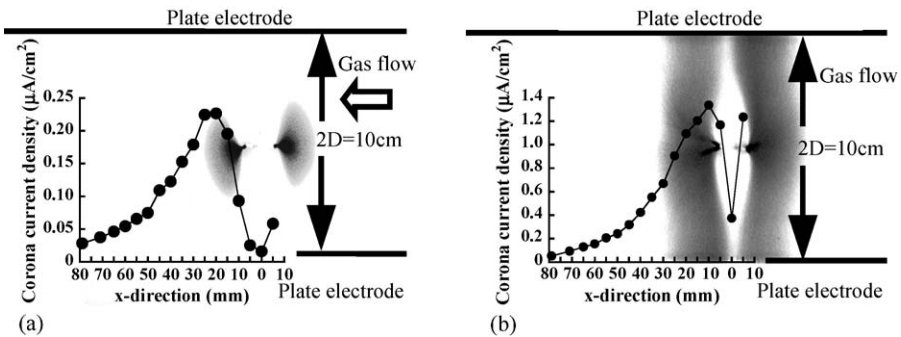


Fig. 5. Comparison of discharge luminescence and corona current density profile ($U_T = 6.7$ mm/s). (a) $V = 17.5$ kV, $I = 14$ μ A, (b) $V = 27$ kV, $I = 85$ μ A.

The current uniformity is improved at higher applied voltage as shown in Fig. 6(d). It is considered that these current distributions affect on the flow field in the reactor.

3.2. Flow visualizations

The airflow around the discharge zone is visualized by using Shadowgraph method. Fig. 7(a) shows schematic side view of the airflow visualization. The effect of heated air on gas flow is negligible as shown in Fig. 7(b). When the discharge is occurred, the streamlines near the stressed electrode become vague due to the turbulent flow around the pipe with nozzles electrode. This is due to the generation of ionic wind from the nozzles. As the applied voltage increases, flow disturbance

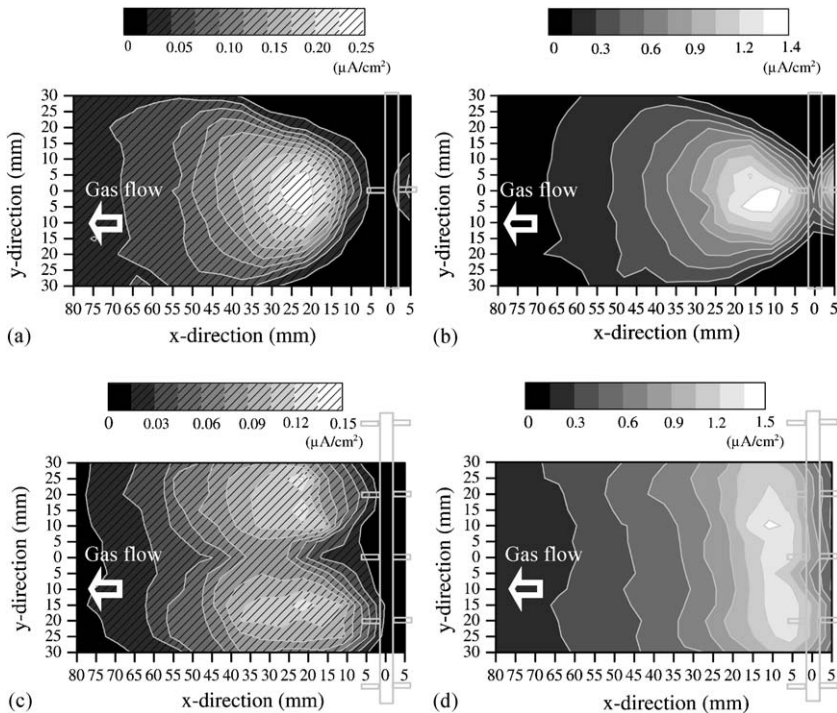


Fig. 6. Corona current distribution on the plate electrode ($U_T=1$ m/s). (a) $V=17.5$ kV, $I=14$ μ A (2 nozzles), (b) $V=27$ kV, $I=85$ μ A (2 nozzles), (c) $V=17.5$ kV, $I=13.5$ μ A (10 nozzles), (d) $V=27$ kV, $I=156$ μ A (10 nozzles)

become significant. These complex airflow patterns observed in this study may correlate with the discharge current distribution caused by the stressed electrode configuration. Moreover, vortex generation can be observed using laser light visualization method as shown in Fig. 8. From these results, it is found that the airflow using the pipe with nozzles electrode is much different from that of the conventional discharging electrode such as the smooth wire. According to the measurement of spatial distribution of ozone in the reactor, the long-live species such as ozone can be transported from the generation area to both downstream and upstream of the discharge region, by diffusion, the additional gas flow from the nozzles and the EHD secondary flow. A mixing of the gas occurs in the reactor, which is a cause of NO removal far from the discharge zone in the upstream.

4. Conclusion

The results obtained are as follows:

1. The corona current distribution depends on the nozzles configuration on the pipe electrode. As the applied voltage increases, the corona current distribution area

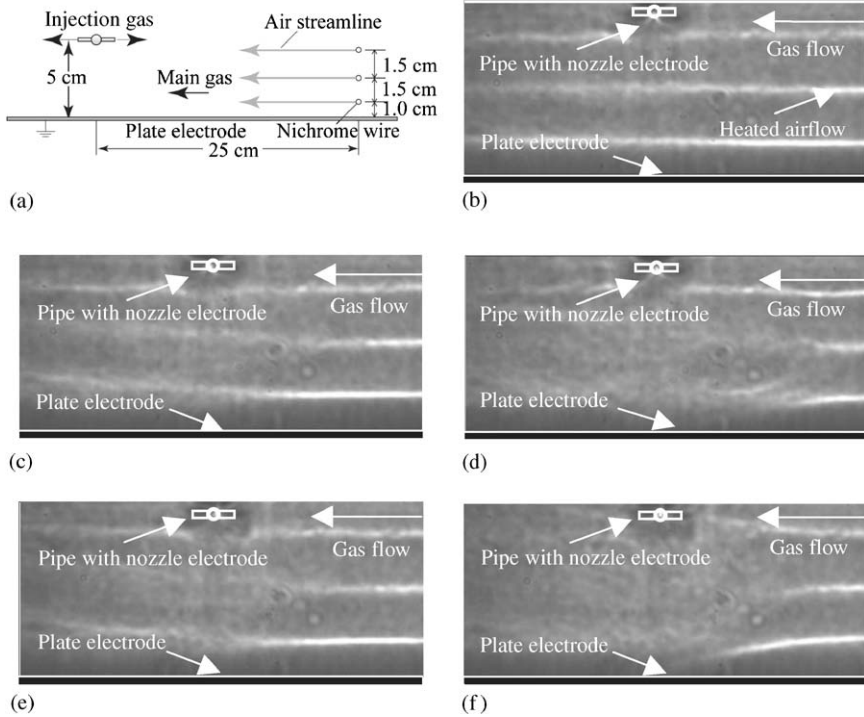


Fig. 7. Shadowgraph images of heated air from upstream heating wires for streamer corona. The white lines in the photographs show stream lines in CRSS ($U_T = 1$ m/s). (a) Schematic side view of the airflow visualization, (b) $V = 0$ kV, $I = 0$ μ A (2 nozzles), (c) $V = 17.5$ kV, $I = 14$ μ A (2 nozzles), (d) $V = 27$ kV, $I = 85$ μ A (2 nozzles), (e) $V = 17.5$ kV, $I = 13.5$ μ A (10 nozzles), (f) $V = 27$ kV, $I = 156$ μ A (10 nozzles).

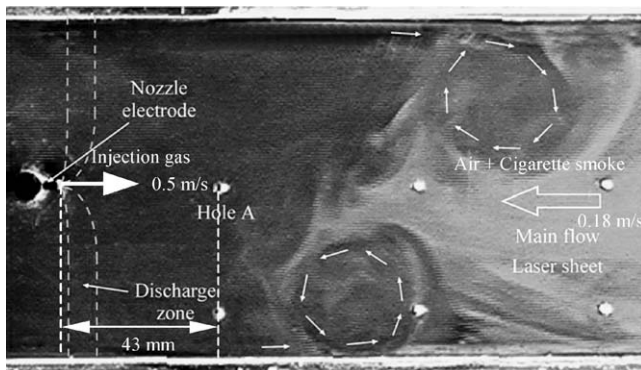


Fig. 8. Image of the flow field in the CRSS reactor using the laser light visualization method ($V = 28$ kV, $I = 150$ μ A, $U_T = 1$ m/s).

increases, while the points of maximum current density reach to the underneath the tip of the nozzles. The current distribution spread much wider than the luminescence area. It is considered that the spatial current flowing to the grounded electrode has an influence on the ionic wind, affecting the airflow around the discharge zone.

2. The airflow observations by Shadowgraph method show the generation of turbulent flow around the pipe with nozzles electrode. These measurements indicate that a mixing of the gas results in enhancement of gaseous treatment if the main gas flow is low.

References

- [1] S. Masuda, H. Nakao, Control of NO_x by positive and negative pulse corona discharges, *IEEE Trans. Ind. Appl.* 26 (1990) 374–383.
- [2] A. Mizuno, K. Shimizu, T. Matsuoka, S. Furuta, Reactive absorption of NO_x using wet discharge plasma reactor, *IEEE Trans. Ind. Appl.* 31 (1995) 1463–1468.
- [3] T. Oda, T. Kato, T. Takahashi, K. Shimizu, Nitric oxide decomposition in air by using nonthermal plasma processing with additives and catalyst, *IEEE Trans. Ind. Appl.* 34 (1998) 268–272.
- [4] T. Yamamoto, M. Okubo, K. Hayakawa, K. Kitaura, Towards ideal NO_x control technology using a plasma-chemical hybrid process, *IEEE Trans. Ind. Appl.* 37 (2001) 1492–1498.
- [5] R. Hackman, H. Akiyama, Air pollution control by electrical discharges, *IEEE Trans. Dielectr. Electr. Insulation* 7 (2000) 654–683.
- [6] T. Ohkubo, S. Kanazawa, Y. Nomoto, J.S. Chang, T. Adachi, NO_x removal by a pipe with nozzle-plate electrode corona discharge system, *IEEE Trans. Ind. Appl.* 30 (1994) 856–861.
- [7] J.S. Chang, J.Y. Park, I. Tomicic, G.F. Round, Simultaneous removal of acid gases from combustion and incineration flue gases by corona radical shower systems, in: *Proceedings of NEDO Symposium on Non-Thermal Discharge Plasma Technology and Air Pollution Control*, Oita, Japan, 1997, pp. 26–37.
- [8] K. Yan, T. Yamamoto, S. Kanazawa, T. Ohkubo, Y. Nomoto, J.S. Chang, NO removal characteristics of a corona radical shower system under DC and AC/DC superimposed operations, *IEEE Trans. Ind. Appl.* 37 (2001) 1499–1504.
- [9] T. Ohkubo, T. Murakami, T. Adachi, Analytic and experimental study of flow field for wire-duct type electrostatic precipitator, *Trans. Inst. Electr. Eng. Japan* 106-A (1986) 377–383.
- [10] T. Ohkubo, S. Hamasaki, Y. Nomoto, J.S. Chang, T. Adachi, The effect of corona wire heating on the down stream ozone concentration profiles in an air-cleaning wire-duct electrostatic precipitator, *IEEE Trans. Ind. Appl.* 26 (1990) 542–549.
- [11] S. Kanazawa, Y. Shuto, N. Sato, T. Ohkubo, Y. Nomoto, J. Mizeraczyk, J.S. Chang, Two-dimensional imaging of NO density profiles by LIF technique in a pipe with nozzles electrode during NO treatment, *IEEE Trans. Ind. Appl.* 39 (2003) 333–339.
- [12] J. Mizeraczyk, J. Podliński, M. Dors, M. Kocik, T. Ohkuubo, S. Kanazawa, J.S. Chang, Electrohydrodynamic Transport of ozone in a corona radical shower non-thermal plasma reactor, in: *International Symposium on High Pressure Low Temperature Plasma Chemistry, Hakone VIII*, Vol. 1, 2002, pp. 78–82.
- [13] P.J. McKinney, J.H. Davidson, D.M. Leone, Current distribution for barbed plate-to-plane coronas, *IEEE Trans. Ind. Appl.* 28 (1992) 1424–1431.
- [14] A. Jaworek, A. Krupa, Corona discharge from a multipoint electrode in flowing air, *J. Electrostatics* 38 (1996) 187–197.